# Opportunities for a graded approach in air sample assay and triage

**Robert B. Hayes[1] and S. Joseph Cope[2]**

[1]North Carolina State University, Nuclear Engineering Department, 2500 Stinson Dr, Raleigh NC, 27695-7909, USA
[2]Joint Base Andrews, 1783 Arnold Ave, MD 20762 USA
Email: rbhayes@ncsu.edu, copesj@nv.doe.gov

***Abstract:***

*Rather than waiting for radon progeny to decay prior to counting an air sample, scalar counts have been shown to provide useful information when appropriate technical interpretation is utilized. This work will review limits from the first frisk of an air sample to recent research showing how the initial decay profile can provide ever increasing discrimination capabilities if measured. Methods demonstrated in the literature along with future opportunities will be reviewed in this presentation. Applications for routine nuclear facility operation, radiological emergency response and treaty verification will also be considered.*

**Keywords:** Air monitoring; Triage; Routine sampling assay

## 1. Introduction

The downwind monitoring of radioaerosols can be used to monitor upwind releases from nuclear facilities. Correlating a measurement to an upwind source can be an arduous task involving many uncertainties and assumptions [1]. One of the physical properties that has to be well understood is the interference created by radon progeny in the air. With radon progeny being alpha, beta and gamma emitters, this can pose various challenges.

Radiological aerosols have additional evolutionary size properties not found in typical organic materials. If these begin as a radioactive gas and have a charged particle decay mode, unique physics can change their subsequent behaviour. Specifically, when the airborne radioisotopes decay by charged particle emission, the resulting atom itself is left with a net charge. This can then induce polarization in any nearby aerosol such that the point charge and the induced dipole have a coulombic attraction allowing them to become attached causing the aerosol to evolve in shape as a function of time and subsequent decays.

Not all radioactive gases with charged particle decay modes will attach to aerosols. This results in an attached fraction and an unattached fraction of the subsequent decay progeny as occurs with radon progeny [2]. The evolution of these radioaerosol particles are then generally sampled with an air filter which itself has particle size sampling efficiencies making precision air monitoring convoluted at best.

### 1.1 Natural sources and decay products from radium

A primary difficulty in radiological air monitoring is due to the ubiquitous and dynamic properties of radon progeny. The crustal content of both $^{226}$Ra and $^{224}$Ra are from their respective $^{238}$U and $^{232}$Th parent primordial decay chains. All $^{226}$Ra and $^{224}$Ra decay into $^{222}$Rn and $^{220}$Rn respectively which are commonly referred to as radon and thoron accordingly. The radon and thoron then have their own decay chains eventually becoming isotopes of lead. These naturally occurring radioactive materials (NORM) have dynamic contributions arising from disparate decay rates, meteorology and regional geology.

The decay series of Radon and Thoron are shown in Figures 1 and 2 respectively

#### *1.1.1 Radon*

The relevant decay series for radon shown in Figure 1 includes maximum beta emission energies. Note that once $^{210}$Pb is formed, it's 21 year half-life effectively removes it from any atmospheric content as it is naturally scrubbed from the air into the soil. The subsequent decay series can be resuspended but generally has a negligible content in air samples.

As radon has a half-life of 3.8 days, it has some time to diffuse out of the host rock which contained its parent $^{226}$Ra. This does require that the noble gas can migrate to a grain boundary or other pathway out of the rock. Even being a noble gas, its generation in the radium inclusions of the host rock do not guarantee a simple diffusion path to the atmosphere. The alpha track damage from the radium decay accumulates over time around these radioactive inclusions and can create at least a portion of a viable path (particularly over time). Recoil from alpha decays of the $^{226}$Ra also cause shorter range local μm scale damage to the mineral matrix. The greater track length of an emitted alpha effectively punches a hole in its host matrix up to many 10's of μm which build up over time resulting in various radial starting pathways for successive radon emanations to travers when randomly attempting to find a grain boundary.

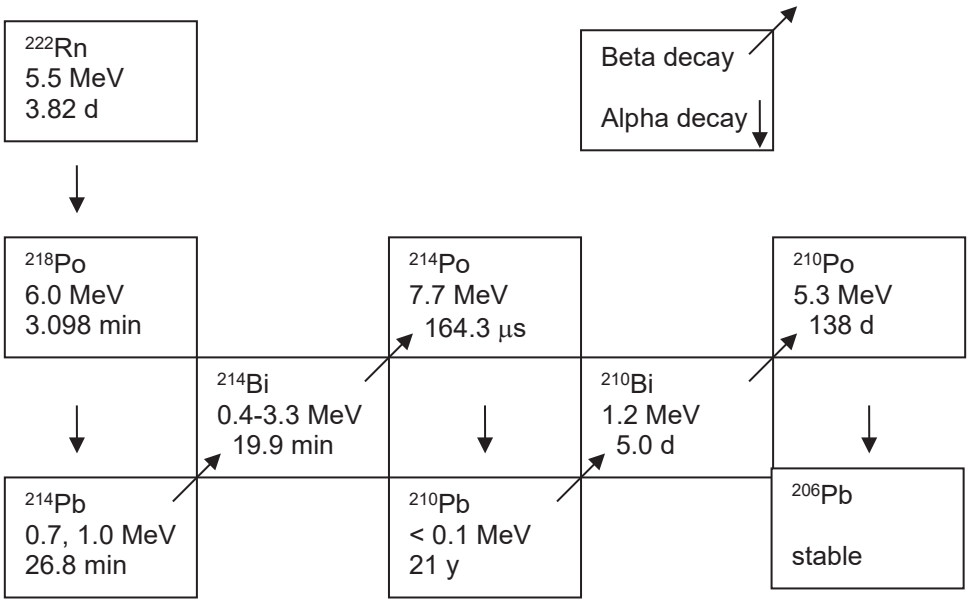


**Figure 1:** $^{222}$Rn decay series (from $^{238}$U), half-lives shown below characteristic energies.

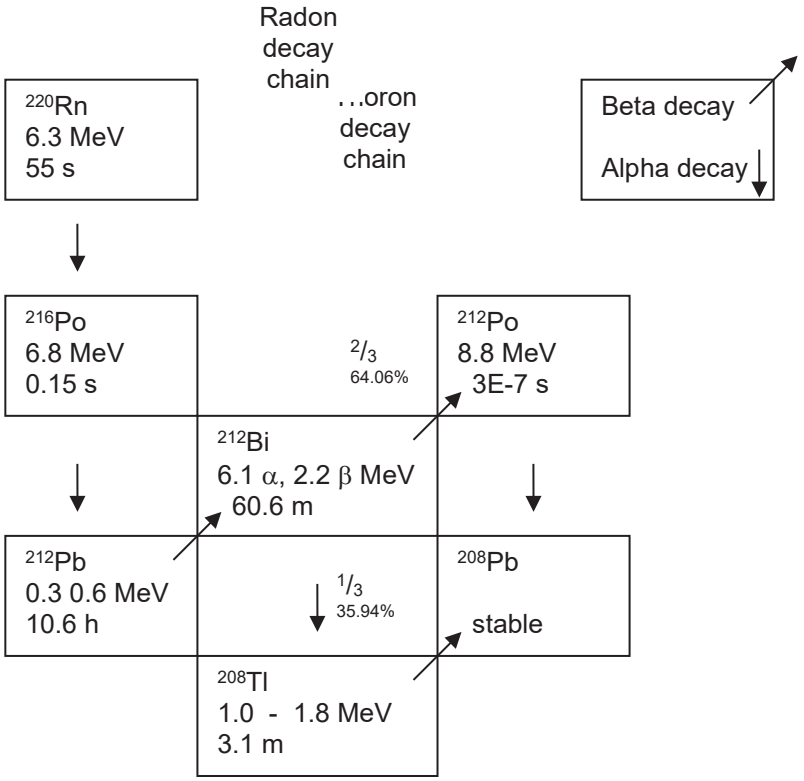


**Figure 2:** $^{220}$Rn decay series (from $^{232}$Th), half-lives shown below characteristic decay energies.

*1.1.2 Thoron*

The thoron decay series is shown in Figure 2 also includes maximum beta energies shown.

Thoron is a bit unique in that its parent $^{224}$Ra along with the primordial $^{232}$Th has a much higher crustal abundance compared to $^{238}$U and its progeny $^{226}$Ra but has a much lower atmospheric content. Although this converse relationship is not expected due to source terms (thoron having a lower air concentration than radon), the actual cause is the half-life of the noble gas $^{220}$Rn which is just under 1 minute. This means that if the thoron is not able to easily escape from the rock matrix into the atmosphere in less than a minute, it will decay back into a heavy metal and so the resultant decay chain is confined to the soil. As such, on average, radon will exceed thoron to around a 3 to 1 ratio even though their parent ratios are inversed.

The thoron decay series has a unique feature of interest in that the isotope $^{212}$Bi is able to decay by either beta or alpha decay with an approximate 2:1 split. This isotope will typically be in transient equilibrium with its longer lived parent $^{212}$Pb when left undisturbed over many hours.

#### 1.1.2.1 Thoron constancy

An additional unique aspect in thoron content is that with the parent having less than a 1 minute half-life, it cannot travel far prior to initiating its decay series. This because radioactivity by nature always has an independent probability of decay so that the portion which arises in gaseous form still has the same half-life as that which was retained in the soil mineral components.

Unlike radon which has a 4 day half-life and can travel great distances with the wind, the 1 minute half-life of thoron does not allow it to travel even nominal distances as it will decay into heavy metals very quickly (Figure 2). The $^{212}$Pb can travel nominal distances having an 11 hour half-life but it is not able to be fed by a continual $^{220}$Rn source as this thoron stays effectively right where it was generated (from $^{224}$Ra decay).

### 1.2 Temporal variations in radon progeny

All the isotopes seen in Figures 1 & 2 are dynamic in that they can be going from attached to unattached (through radioactive decay recoils and gaseous collisions) along with the parent gaseous isotopes going through increases or decreases from other effects. These changes can all contribute to the variations seen in this interfering background radon progeny distribution. Understanding the various causes for these changes can allow mitigation, controlling or otherwise addressing any deleterious effects from the same. An example of a typical alpha and beta spectrum from ambient air showing the various naturally occurring airborne radionuclides is seen in Figure 3.

#### *1.2.1 Causal initiators of radon progeny dynamics*

There are many factors which give rise to variations in natural airborne radioactivity levels. The largest tends to be that of temperature inversions. A natural inversion typically occurs in the mornings due to the adiabatic lapse rates from the ground preventing any mixing of surface air with the upper atmosphere. This means that all radon which has escaped from the ground simply builds up near the surface until it can be diluted later in the morning due to convective currents which allow mixing with the upper atmosphere. These convective currents are initiated by ground heating from solar irradiance in the morning. This effect also has seasonal dependencies with winter typically having the largest inversion effects resulting in the largest ground radon concentrations.

Another very large effect in environmental radon and its progeny comes from precipitation. When rain falls through radon and its progeny it pushes these radionuclides to the ground cleaning the air but raising the terrestrial dose rate by many orders of magnitude [3]. Barometric pressure is another cause of changing radon levels. When a low pressure comes in, this can pull radon from the soil as a high pressure system can retard radon diffusion from the ground.

### 1.3 Alpha and beta spectra from environmental samples

The distribution of energies shown in Figures 1 and 2 result in spectra exemplified by Figure 3 where no transuranic (TRU) activity is present. Here, the peaks are labelled by their dominant contributing radionuclides. The peak location represents those occurrences when emitted alpha particles move normal to the filter and detector depositing a characteristic energy into the detector active volume. Spreading occurs from interstitial air, filter media and oblique paths to the detector from the source filter. In this sense, the majority of detected alpha particles is not at the maximum possible energy for a particle where minimum attenuation takes place in the filter, its sampled material, the air layer separating the detector and the detector dead layer.

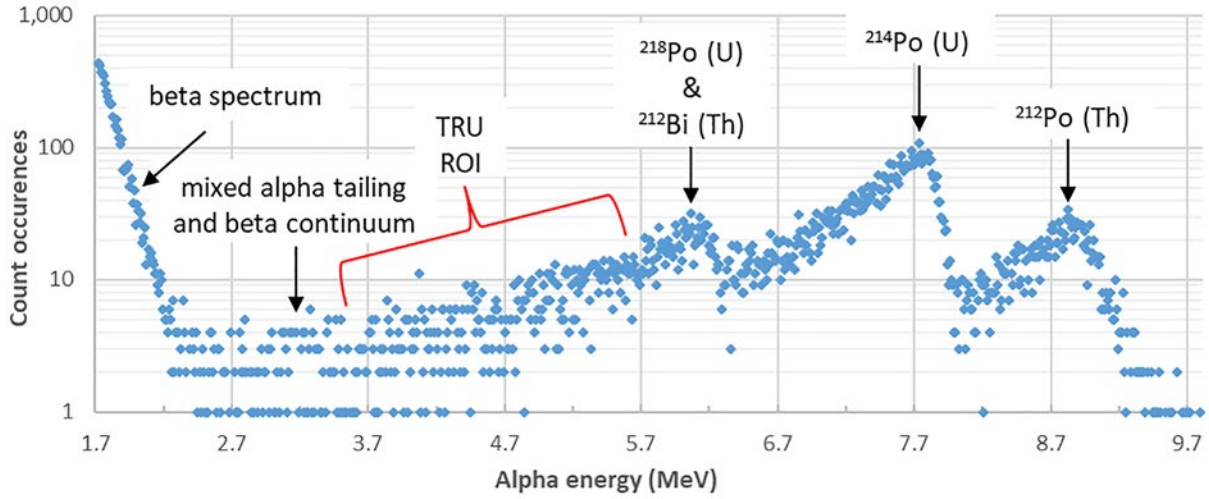


**Figure 3:** Example charged particle spectra (semi-log) measured from an environmental air sample with peaks and regions labelled associating primordial parents indicated as $^{238}$U=U and $^{232}$Th=Th from Figures 1 & 2.

The TRU region of interest (ROI) in Figure 3 represents where most of the transuranic isotopes will be present and so the large count rate present from tailing of the higher energy NORM alpha peaks creates considerable background in the TRU ROI (hence the desire to allow them to decay prior to assay).

The abscissa scale is based on only the three labelled NORM peaks so that the beta energies are overestimated in this scheme. This is because the ionization in the detector has a higher efficiency with beta particles than alphas for the same kinetic energy. Alpha particles lose a certain portion of their energy creating vacancies and interstitials due to recoiling nuclei whereas beta particles have a much higher threshold to displace an atom in the detector volume resulting in a larger fraction of their deposited energy going into ionization only.

*1.3.1 Spectral manipulation options*

Typical commercial options to mitigate these features involve curve fitting the shapes which is feasible when substantial particulate loading does not drastically degrade the spectra from self-attenuation effects. The more complicated options include Gaussian fits to the top of the peaks with exponential tails above and below these. Other options include simple region of interest (ROI) summing of the peak areas separated by their respective minima. Template shapes for each peak could be fit in amplitude as well but each of these options have potential issues with spectral degradation occurring as filter loading increases (due to dust build-up).

Peak shifting and tailing slope dependencies with filter loading could be mitigated by allowing peak locations to be variables along with exponential fitting portions (or template shapes). This would require sufficient knowledge of overlap dependencies in the TRU ROI for discrimination purposes.

1.3.1.1 Limitations with spectral manipulation

When filter loading occurs, the peak locations shift to lower energies and the low energy tails from each peak will increase accordingly. The low energy tails seen in Figure 3 can be verified upon inspection that they would all match an exponential function well (due to the linear appearance in the semi-log format). The argument of the exponential in such a fit would then be functionally dependent on the filter loading in a potentially predictable manner with sample mass (assuming linear deposition rates). Similarly, the peak locations could also be functionally dependent on filter loading. In principle, dependencies such as these could be monitored and trended to estimate filter loading and so serve as a metric for when to change a filter and so optimize sample sensitivity overall.

It should be pointed out that there are some TRU isotopes having energies near the 6 MeV NORM peak, specifically, the $^{252}$Cf and some of the curium isotopes, such that these have peaks very near or even indistinguishable from the 6 MeV NORM peak. Methods to mitigate this are discussed in a later section but invariably utilize the decay series (see section 1.3.2) in some fashion.

**1.3.1.2. Potential benefits from spectral analysis**

In principle, sensitivity could be increased over gross counting given that each alpha emitter has distinct ROIs which follow defined patterns which could be leveraged in the analysis using various means. If the contributions to the TRU ROI can be accurately estimated from the higher energy NORM peaks, then the background in this ROI can be substantially decreased and so concomitantly decrease the detection limit for anthropogenic activity. If spectral quality metrics are designed to indicate when the assumptions from the fit are being challenged, then additional rigor in the assay can be realized. Care should be utilized in any such approach as vendors have historically fallen short in properly testing and validating such systems prior to marketing.

*1.3.2 Spectral and temporal coupling*

The decay series given in Figures 1 & 2 all have to obey the Bateman equations represented by Equation 1. These are the governing equations for all radioactive decay series allowing for any length of a decay chain. Here each isotope activity $A_j$ has an associated decay constant $\lambda_j$ with an initial parent concentration $N_1(0)$.

$$A_j(t) = N_1(0)\sum_{m=1}^{j} C_m e^{-\lambda_m t} \text{ where the coefficients}$$

$$C_m = \frac{\prod_{i=1}^{j}\lambda_n}{\prod_{\substack{i=1\\ j\neq m}}^{j}(\lambda_i - \lambda_m)} \qquad (1)$$

1.3.2.1 Decay characteristics for thoron 6 MeV alpha contribution

This means that the standard decay rate of the $^{212}$Bi alpha peak at 6.1 MeV will be fed by the decaying $^{212}$Pb isotope which is easily discriminated by it's associated isolated 8.8 MeV peak from the subsequent progeny $^{212}$Po. Due to the negligible half-life of $^{212}$Po, it is continually in transient equilibrium with its parent $^{212}$Bi scaled only by the appropriate beta branching ratio of the latter.

1.3.2.2 Decay characteristics for the radon 6 MeV alpha contribution

Likewise, the radon progeny contribution to the 6 MeV peak from the $^{218}$Po initial activity is itself the source of contributing activity to the initial $^{214}$Pb activity which contributes to both of the initial $^{214}$Bi and $^{214}$Po activities with the latter emitting the readily discriminated 7.7 MeV peak. Specifically, due to the negligible half-life of $^{214}$Po, it is

always in transient equilibrium with its parent $^{214}$Bi. From these, the Bateman equations (Eq. 1) could be used (explicitly or through some simplification) to correlate background in the TRU ROI (from $^{218}$Po contributions) to the readily discriminated count rates in the $^{214}$Po ROI (this would likely be a retrospective or delayed correction).

*1.3.3 Beta spectral options*

The beta portion of the spectrum can be folded into any desired use of the Bateman equations (Eq. 1). Typically, the radiological risk from beta activity is so much lower than that of TRU alphas that gross counting is adequate to provide desired detection sensitivity [4]. As such, the exact beta energy calibration is not considered of high importance given its added difficulty of only having a continuum source preventing a simple and precise means of scaling (particularly in the presence of alpha cross talk).

### 1.4 Mitigating radon progeny in air monitoring

Typical air monitoring techniques involve pulling a precisely measured volume of air through an air filter. The air filter is then assayed for radiological content such that the ratio of the assay to the volume is the resultant air concentration ascribed to the space sampled. The standard approach utilized in routine nuclear operations, radiological emergency response and even treaty verification is to allow the air sample to sit for multiple days to allow the entrained radon progeny to decay prior to characterizing any anthropogenic content on the air filter. This is due to the array of alpha, beta and gamma disintegration energies present in any aged sample of ambient air due to all the radon progeny present (Figures 1, 2 and 3).

In principle, the air sample could be measured at any time while waiting for the radon progeny to decay away, but unless the anthropogenic component is large compared to the radon progeny, discrimination is haphazard at best. Vendors have claimed to produce algorithms which can discriminate anthropogenic activity based on alpha and beta spectrometry which have been shown to be unreliable [5,6].

*1.4.1 Initial frisk*

Based on the ratio of alpha to beta activity, some limits can be placed on the maximum anthropogenic which can be present and still attain these ratios [7]. Given that radiation cannot be sensed in any of the traditional observational modes (sight, smell and touch), it requires detectors and so airborne radioactivity, when present, requires similar infrastructure. The variability in alpha to beta ratios can vary dramatically due to all the dependencies on the contributing isotopes (see section 1.2). All that the initial frisk can determine is whether the ratio of alpha activity to beta activity could credibly have been obtained from the normal variability in NORM.

1.4.1.1 Mitigation limitations

Any initial frisk values will by definition be dynamic and so generally very insensitive in discriminating NORM from anthropogenic. The various combinations of attached and unattached fractions coupled with dynamic radon and thoron levels with size dependent filter efficiencies etc all couple into a difficult characterization at best.

This is problematic in that virtually all air samples have only trace quantities of the target isotopes unless only radon progeny itself is being assayed. This trace characteristic inherent to the isotopes of interest in an air sample arises from the nature and purpose of the sample. In normal operations, most air samples are intended to demonstrate either a zero release or at most a regulatory compliant result (which is always small).

In emergency response, field teams would have to dress out in full personnel protective equipment along with decontamination of vehicles if they were to sample in contaminated areas. As such, field teams typically sample on the penumbra of a plume so that the contamination levels are comparable to background already making detection difficult (where the bulk of any release or ground deposition characterization occurs from the air with large gamma detection arrays).

Treaty verification is generally very far down range again making concentrations almost vanishingly small. In all cases then, the radon progeny on an air sample is likely to be the dominant source of all ionizing radiation emissions.

### 1.5 Utility of the presented methodologies

The research reviewed in this work demonstrates novel methods to characterize the anthropogenic activity in such a way as to utilize the interferent radon progeny signals to estimate the long lived activity on the filters. Rather than throw away these interferent signals, this work will review various means to use them in a graded approach to characterizing airborne radioactivity. In this way, rapid, yet quality, initial TRU estimates can be obtained in any air sample protocol from treaty monitoring to nuclear safety and even operational radiation safety applications.

## 2. Graded approach

The graded approach itself means that improving levels of quality will scale with increasing effort or time permitting defence in depth towards the eventual goal. In this case, we are looking for a quality method to characterize anthropogenic radionuclide levels in the atmosphere despite the interfering radon progeny species. Quality being defined here as a measurement containing rigorous physics based characterization of the true dispersion inherent to the final assay results.

The current missing piece in air monitoring data is a quality assay technique which can be used to characterize air samples while the radon progeny is still relatively high. Provided that the uncertainty estimates are rigorous and accurately describe the dispersion in the measurements, high uncertainty values are entirely useful. This is because some quality information is always better than no information where quality is strictly defined as any assay having rigorous uncertainty estimators.

### 2.1 Quality convergence

The intent for air monitoring is to properly characterize the risks associated with airborne materials. With radiological materials, this is typically the risk from inhalation which is measured in actual or potential dose. Potential dose being the dose a person would receive were they to actually be in a given location for a proscribed period of time (such as a theoretically maximally exposed individual). Consequences can also be in terms of land contamination which again is typically measured in terms of risk by the maximum potential dose an individual could credibly receive from all input vectors. With treaty compliance monitoring, the desired result is not just detection but discrimination from legitimate commercial sources.

#### *2.1.1 Nuclear security*

In nuclear emergency response, treaty verification and even non-proliferation applications, quality may be measured in at least two ways. In some sense, characterization of any anomaly would be inherently useful enabling further investigation. In a more detailed example, quality may be expressed in terms of the rigor with which the anthropogenic portions of the air sample can be ascribed to adversary behaviour and discriminated from legitimate industrial or commercial endeavours. It is in the discrimination of adversary actions from those beneficial activities that is needed in nuclear security applications.

Current technology largely relies on chemical, nuclear and morphological assays from air sample particulate. As with all of the other air monitoring applications, the radiological characterization portion requires mitigation of the natural radon progeny inherent to all commercial air sampling technologies.

## 3. Using all the decay data

When allowing the radon progeny to decay prior to the resultant air sample assay, it is inherently assumed that the progeny is purely an interferent and so does not contain useful information regarding the target assay of the anthropogenic activity. Our research has shown that there is useful information which can be extracted from the natural radon progeny when evaluated in a graded approach formalism. Specifically, starting with a quick handheld frisk for a very low quality assay (assuming a frisk has known efficiencies [7]), some information can be obtained. Additional measurements when continually applied (utilizing appropriate instrumentation and analysis) allows a continual improvement in the precision of assays (without compromising accuracy) until the eventual “gold standard” of destructive assay by radiochemistry can be applied some days or weeks later. The key is being able to use the physics of the interferent to help characterize it and so subtract or mitigate it in some useful way.

### 3.1 Decay curve fitting

In principle, all radioactive decay chains adhere to the Bateman equations (Eq. 1) which can address only radioactive decay. If the initial conditions are known, then the Bateman equations can be solved to predict all isotopic abundances in the decay chain for all future times. Radon progeny has the inherent difficulty that the parent is continually changing (see section 1.2) and meteorological changes can also drastically bias progeny separate from the radon parent. This being partially due to the parent being a noble gas with the progeny being heavy metal (ions) either attached or unattached to ambient aerosols.

If the Bateman equations were utilized, their general form would follow that given in Equation 1 such that fitting to a measured series of counts (a decay curve) could result in an overdetermined system of equations. With radon having only 4 relevant radioactive progeny (Figure 1) and thoron having 5 (Figure 2), this would require at a minimum of 9 decay count measurements to obtain estimates for each isotope initial activity estimate. If only 9 counts were obtained, measurement scatter would prevent an exact fit despite 9 fitting parameters attempting to model 9 data points as Equation 1 can only model continuous and smooth functions and so not noise.

#### *3.1.1 Curve fitting statistics*

Due to instrument uncertainty and statistical fluctuations in decay rates, at least a dozen or so measurements are desired for each degree of freedom to approximate a normal distribution in the fitted parameters convergent value. With this number of data points, a mean, its standard deviation along with a chi-squared test to evaluate the likelihood that the distribution was normal can all be estimated for any given parameter. When multiple parameters are being estimated in a curve fit, commensurately more data points would be desired. If only 2 parameters are to be estimated (an initial activity and a decay constant), then preferentially more than a dozen measurements would be the target.

This approximation assumes that around ten measurements are desired for a single mean, and a few dozen for a line and around 30 for a quadratic and so on. There is no hard limit or rule for such a generalization but the driver here is to get a quality *t*-test on each fitted parameter. A quality *t*-test is not dependent on sample number if the

assumption of normality is valid. Estimating normality based on a small sample is largely untenable so this gross assumption is stated as a matter of opinion only.

*3.1.2 Overdetermined curve fits*

Technically, one can estimate the slope, intercept and their uncertainties along with a standard error of the fit and a correlation coefficient from just 3 points (even random points). In this extreme example, 5 values are obtained from 3 data points giving an apparent negative set of degrees of freedom. This really just means that multiple measures of the mean and distribution are redundant and do not convey independent information despite their typical interpretation being independent measures of central tendency.

One general goal in curve fitting is to increase your degrees of freedom as much as possible without excessively incurring scatter by splitting up your counting interval into ever decreasing intervals. Using the traditional definition of degrees of freedom (*DoF*) being the difference between the number of fitted data points (*N*) and that of the number of fitting parameters (*M*), it is preferable to have this value (*DoF=N-M*) as close to 30 as possible to enable an assumption of normal statistics. Otherwise, a *t*-distribution would be assumed incurring less certainty in distribution types (which can itself be tested).

### 3.2 Radon progeny decay curves

The two dominant isotopes driving the decay rates from radon progeny are the $^{214}$Pb and $^{214}$Bi isotopes having half-lives of 26.8 m and 19.9 m respectively (Figure 1). Combining these two in sequence via Equation 1 results in an approximately effective decay constant greater than either producing values ranging from 30 to 40 minutes (depending on initial conditions).

In order to get proper leverage in measuring the half-life of a radionuclide through a decay curve, ideally the measurement time should be long compared to the half-life. If a large section of the effective decay curve from radon progeny is to be sampled, then ideally at least 30 minutes of sampling time would be a minimum.

### 3.3 Long lived activity decay curves

If an operationally friendly time window for measuring an air sample is a few hours, then any activity having a half-life large compared to this would appear to be largely indistinguishable from a constant. Here, an isotope with constant activity does not actually exist but can be approximated by any radionuclide with a very long half-life compared to the count time.

With this, if thoron content is present in an air sample which only measures decay over a period of a few hours or less, the 10.6 hr half-life of $^{212}$Pb would cause it to look like constant (anthropogenic) activity like that of a transuranic (TRU) nuclide. If a decay curve fit modelling the radon progeny did not account for this thoron content in a short time window, this component would conservatively bias the long lived (approximately constant) activity to have a higher estimate.

### 3.4 Combined decay curves

If a decay curve is measured within a few hour window, the radon progeny would appear to go through multiple half-lives while the thoron progeny would appear largely constant. Any anthropogenic activity present will likely have decay constants comparable to $^{137}$Cs, $^{90}$Sr or any of the TRU nuclides which effectively would be modelled as a constant activity. Putting all this together in a decay curve fit model, Equation 2 presents the filter activity $A(t)$ at any given time $t$ following flow cessation. Here, $m1$ is the initial short lived activity, $m2$ is the effective short lived decay constant and $m3$ is the long lived activity which will be biased high due to thoron progeny. If this function is then fit to a decay curve, the effective half-life is then $\ln(2)/m2$. All results used the Levenberg-Marquardt fitting algorithm to data.

$$A(t) = m1 \times e^{-m2 \times t} + m3 \tag{2}$$

## 4. Historical results

When fitting actual filter decay data, the distribution seen in Figure 4 was obtained as described elsewhere [8]. The distribution shown represents the suite of resultant $m3$ values and their uncertainties combined via a kernel density estimator. The results from plutonium superposition with environmental air samples is shown on the left with a similar thorium study shown on the right. In these works, the results from using Equation 2 on actual air filters both with and without anthropogenic activity are compared in their rapid assay capabilities.

The histogram results shown in red are the calibration results obtained from filters not having any interferent NORM activity representing the correct values and their distribution which should be obtained from a proper use of Equation 2 on air filters having both interferent natural and anthropogenic activity.

The blue histogram results were obtained using Equation 2 on filter decay counts which had both the anthropogenic and natural radioactivity constituents. The two distributions (red and blue) are visually indistinguishable although the histogram results do not incorporate individual measurement errors from fitting Equation 2 to the decay curve data.

The red and blue dashed vertical lines represent the mean from each distribution. In this sense, the blue is the best estimate from the fitting approach of Equation 2 to environmental air samples with a TRU source superposition. The TRU source distribution without radon progeny activity is shown in red. What is evident from the blue data is that

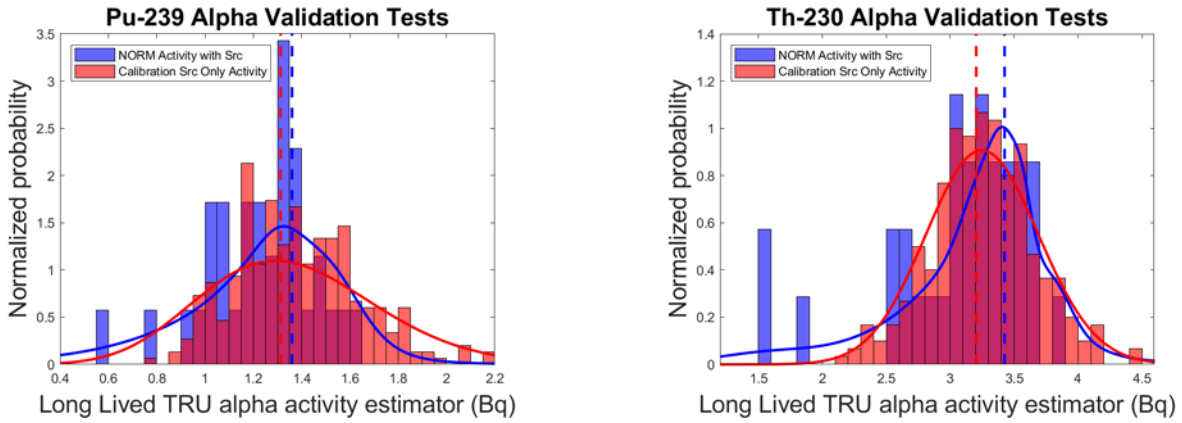


**Figure 4:** Decay curve fit results from effectively spiked air filters [8]. Blue values represent a used air filter superimposed with TRU activity. The red values represent blank (unused) filters superimposed on the same TRU activity used in making the blue results.

on average, use of Equation 2 provides conservative estimates of the known anthropogenic activity (indicated by the red data).

### 4.1 Kernel density estimator (KDE)

When histogramming data possessing individual uncertainties, the uncertainty portion of the data is simply discarded. This need not be the case when using a KDE which is represented by Equation 3. This effectively turns each data point used to construct the histogram into a normalized Gaussian so that the superposition of all these Gaussians becomes a continuous probability distribution function when Equation 3 is used to represent the data. This allows deconvolution of the resultant KDE into individual components or to conduct hypothesis testing on the resultant distribution. Note that the parameters used in Equation 3 are such that $\mu_i$ are the individual measured values having unique uncertainty values of $\sigma_i$ from $n$ total measurements. The use of $P(x)$ is intended to convey that when normalized in this way, the KDE is a proper probability density function sufficient for hypothesis testing.

$$KDE(x) = P(x) = \frac{1}{n}\sum_{i=1}^{n} \frac{e^{-0.5\left(\frac{x-\mu_i}{\sigma_i}\right)^2}}{\sigma_i\sqrt{2\pi}} \qquad (3)$$

The KDE values from the fitted $m3$ distributions (Equation 2) are presented in Figure 4 as continuous lines which are color-coded in conjunction with the histograms.

### 4.2 Upper confidence limit of individual fits

The blue results seen in Figure 4 clearly have entries which are below the red dashed line. With the red vertical dashed line representing the correctly calibrated (best estimate) of the TRU content measured with the air filters, the lower blue occurrences would be underestimates and so not a conservative assay. As such, this might appear to give results which when using Equation 2 would underestimate the correct anthropogenic activity and so constitute a potential safety concern. This turns out not to be the case when individual measurement results are evaluated at their upper 95% confidence limit. When taking all the assayed results at their upper 95% CL, there were no underestimates of the characterized TRU source activity found demonstrating the savings offered from fitting decay curves using Equation 2 allowing for conservative upper bounds in all observed cases.

A histogram of all the measured assays of the TRU content using Equation 2 are shown in Figure 5. Here, the results shown are all of the $m3 + 1.645\sigma_{m3}$ values obtained previously [8].

Previous work has considered 30 min intervals within a 2 hr counting window to understand the uncertainty penalties associated with more rapid TRU activity estimation; again, the results can still be considered quality, even with a large uncertainty estimator, provided that it is rigorous and maintains a physical basis. Utilizing a weighted average of 35 filters for each TRU source study, the TRU estimate for each time study is given in Figure 6. The error bars noted in Figure 6 represent the standard error of the mean at the 95% CL and should be interpreted as a potential "best estimate" scenario when conditions allow for a weighted average technique. What is truly profound is that this conservatism remains throughout the range of 30 minutes up to 2 hr measurement time with shorter measurement intervals incurring larger uncertainty (and so higher conservatism in the upper 95% CL) as reported elsewhere [9].

These results show that the asymptotic constant activity value at infinity from Equation 2 results in conservative estimates of the long lived activity whenever uncertainties are evaluated at the 95% CL. This is attributed to both the thoron progeny bias ($^{212}$Pb limiting the $^{212}$Bi activity change in rate) when measuring a short time interval and taking only the upper 95% CL. In this thoron progeny bias, the $^{212}$Bi alpha and beta decays approach a transient equilibrium with the parent $^{212}$Pb activity which has just under an 11 hour half-life.

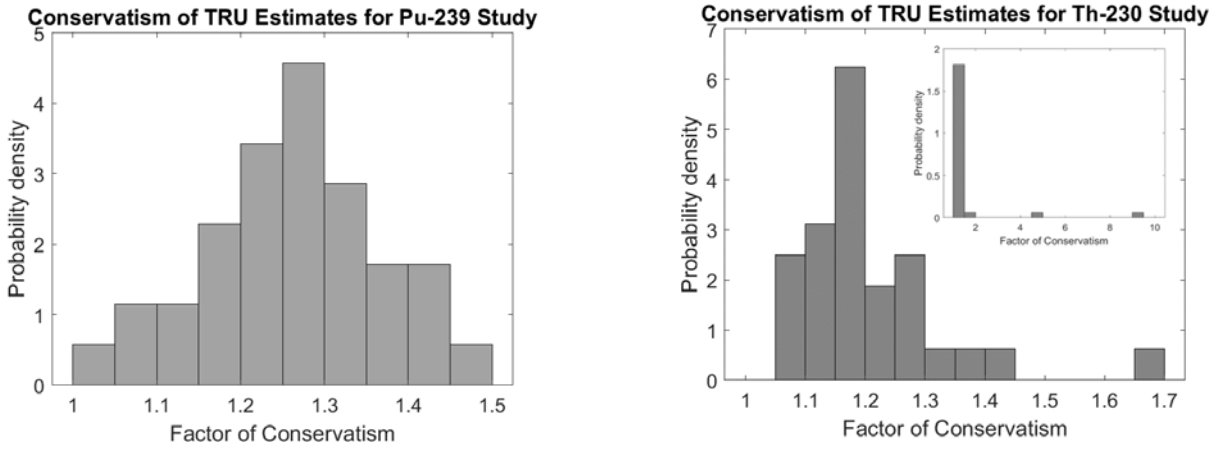


**Figure 5:** Upper 95% confidence level obtained from using Equation 2 to rapidly estimate anthropogenic content on air filters [8]. Values include thoron progeny bias from conducting only a 2 hour decay count.

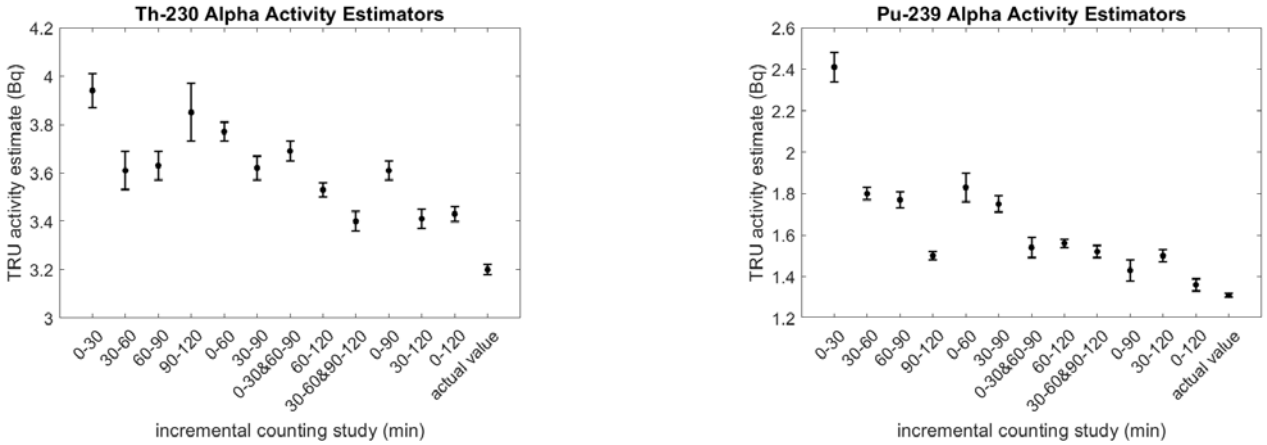


**Figure 6:** Incremental 30 min weighted average TRU alpha activity estimates from effectively spiked environmental air filters with uncertainties shown as standard error of the mean [9].

### 4.3 Summary of results

The decay curve fitting of sequential count data using the Levenberg-Marquardt algorithm can provide parameter estimates with their associated uncertainties to Equation 2. This enables novel applications involving kernel density estimators and their subsequent deconvolution [10]. More importantly, multiple options for using the information normally discarded in traditional air sampling assay has been shown to give quality low precision results quickly [9]. This in turn fills a high priority information gap typically occurring when air concentration data is desired rapidly from standard air samples.

#### 4.3.1 Alternative approaches to triage

Many other options for pursuing further graded approaches in air sample assay and triage have been identified beyond the results reported here [11,**Error! Reference source not found.**2]. These generally involve spectroscopy coupled with other methodologies but can even include additional gross assay techniques (such as longer count times). The spectral analysis methods could even include mass loading mitigation, temporal dependencies and assaying of TRU isotopes having the insidious alpha decay energies very near 6 MeV.

## 5. Discussion

The KDE results seen in Figure 4 would permit deconvolution into the respective error contributing sources. Previous results have been able to discriminate contributions from the instrument and those of radon and thoron [10]. The techniques described here demonstrate utility in the period of time while samples are customarily being allowed to passively decay away to clear up the TRU ROI signals seen in Figure 3 and so allow low detection limits.

### 5.1 Emergency response applications

In emergency response scenarios, this could be accomplished when samples are being returned from the field. Having a small scalar or spectral counter in the transport vehicles would allow obtaining results prior to submitting samples to the lab. Starting with an initial frisk, the samples could be continually counted in a decreasing uncertainty manner allowing quality triage in determining which samples should be shipped off for formal radiochemical digestion, separation, electroplating and final vacuum alpha and beta spectroscopy (a high resolution version of Figure 3 with no radon progeny present).

### 5.2 Treaty verification applications

Modern Comprehensive Test Ban Treaty (CTBT) monitoring based on the Radionuclide Aerosol Sampler/Analyzer (RASA) systems require a delay in assaying radioaerosols to allow radon progeny decay. If a large release just went past a monitoring station, it would have to wait for the decay period to elapse prior to even looking for the activity. The discussed approach involving decay curve fitting could be accomplished as a low sensitivity interim measurement enabling this early warning capability for any nominal plume passage prior to the customary wait periods.

### 5.3 Operational health physics applications

Nuclear facilities routinely allow air samples to lay dormant prior to measurement to remove radon progeny through decay. If early estimates were desired, fitting the decay curve would allow just such a graded approach to their defence in depth. Simply put, quality assays can be obtained rapidly if desired.

## 6. Conclusions

Many opportunities to improve standard air sample analysis have been explored with examples provided of some of those which already have experimental results. Utility of the decay curve fitting methodologies appear to have potential application in nuclear safeguards, non-proliferation, radiological emergency response and even routine health physics applications.

## 7. Acknowledgements

This material is based upon work supported by the Department of Energy National Nuclear Security Administration under Award Number(s) DE-NA0002576. Additional support of this work was through a joint faculty appointment between North Carolina State University and Oak Ridge National Laboratory in coordination with the Office of Defence Nuclear Nonproliferation R&D of the National Nuclear Security Administration sponsored Consortium for Nonproliferation Enabling Capabilities (CNEC) with additional support from the Nuclear Regulatory Commission grant NRC-HQ-84-14-G-0059.

## 8. References

[1] Hayes RB. Reconstruction of a radiological release using aerosol sampling Health Phys. **112**(4), p 326-337; 2017.

[2] NCRP, National Council on Radiation Protection and Measurements. Radon exposure of the U.S. population, status of the problem. Bethesda, Md: National Council on Radiation Protection and Measurements; 1991;1990;.

[3] Mercier JF, Tracy BL, d'Amours R, Chagnon F, Hoffman I, Korpach EP, Johnson S, Ungar RK; *Increased environmental gamma-ray dose rate during precipitation: a stong correlation with contributing air mass*; Journal of Environmental Radioactivity; **100**; p 527-533; 2009.

[4] Code of Federal Regulations; *Derived Air Concentrations (DAC) for controlling radiation exposure to workers at DOE facilities*; 10 C.F.R. § 835 Appendix A; 2011.

[5] Hayes RB; *False CAM Alarms from Radon Fluctuations*; Health Phys; **85**; p S81-84; 2003.

[6] Hayes RB; *Problems found using a radon stripping algorithm for retrospective assessment of air filter samples*; Health Phys; **94;** p 366-372; 2008.

[7] Justus AL; *Prompt Retrospective air sample analysis – A comparison of gross-alpha, beta-to-alpha ratio, and alpha spectroscopy techniques*; Health Phys; **100**-2**;** p 191-200; 2011.

[8] Cope SJ, Hayes RB; *Validation of a Rapid, Conservative Transuranic Alpha Activity Estimation Method in Air Samples*; J Radiolog. Prot **39**, 749-765 doi.org/10.1088/1361-6498/ab1bfd.

[9] Cope SJ, Hayes RB; *Incremental Gains in Transuranic Activity Analysis in Air Samples for Radiological Emergency Response*; Nuc Tech; . DOI: 10.1080/00295450.2019.1590074.

[10] Cope SJ, Hayes RB; *Preliminary work toward a Transuranic Activity Estimation Method for Rapid Discrimination of Anthropogenic from Transuranic in Alpha Air Samples*; Health Phys; **114**-3; p 319-327; 2018.

[11] Konzen K, Brey R; *A method of discriminating transuranic radionuclides from radon progeny using low-resolution alpha spectroscopy and curve-fitting techniques*; Health Phys; **102**; p S53-S59; 2012.

[12] Pollanen R, Siiskonen T; *Minimum detectable activity concentration in direct alpha spectrometry from outdoor air samples: continuous monitoring versus separate sampling and counting*; Health Phys; **90**; p 167-175; 2006.